Thin Solid Films 519 (2011) 2604–2607

Contents lists available at ScienceDirect

Thin Solid Films

journal homepage: www.elsevier.com/locate/tsf

Free-charge carrier profile of iso- and aniso-type Si homojunctions determined by terahertz and mid-infrared ellipsometry

A. Boosalis [a,*], T. Hofmann [a], J. Šik [b], M. Schubert [a]

[a] Department of Electrical Engineering, University of Nebraska-Lincoln, Lincoln, NE 68588-0511, USA
[b] ON Semiconductor, Rožnov pod Radhoštěm, Czech Republic

ARTICLE INFO

Available online 10 December 2010

Keywords:
Terahertz
Isotype
Homojunction
Silicon
Spectroscopic ellipsometry

ABSTRACT

We present an optical, non-destructive, non-contact method of determining the silicon homojunction epilayer free-charge carrier concentration profile and thickness by means of combined terahertz (0.2–1 THz) and mid-infrared (10–50 THz) spectroscopic ellipsometry investigation. A dual homojunction iso- and aniso-type silicon sample is investigated. Application of analytical models for iso-type and aniso-type homojunctions results in an excellent match between calculated and experimental data. Best-match model calculated parameters are found to be consistent with electrical spreading resistance epilayer thickness and resistivity values.

© 2010 Elsevier B.V. All rights reserved.

1. Introduction

The ability to mathematically model and measure the electrical and structural properties of homojunctions lies at the core of many imminent technologies. As on chip communications demand lower power and higher speed processes, engineers look to homojunction structures for integrated circuit waveguides and optoelectronic modulators [1,2]. For example, homojunction interfacial work function internal photoemission (HIWIP) far-infrared detectors utilize iso-type homojunctions and offer tunable spectral ranges and well known silicon manufacturing technologies [3].

Iso-type and aniso-type homojunctions are characterized by electric free-charge carrier (FCC) interactions at the junction interface. In each case it is assumed that dopant atoms have zero mobility, so the steady state electric charge distribution is due entirely to FCC action. An aniso-type homojunction is a material junction where the crystalline bulk (e.g., silicon) is identical on either side of the junction in crystallographic orientation only, but possesses doping materials of opposite carrier types and different doping concentrations. This type of junction is also known as a p-n junction, or a diode. The FCCs of opposing sign create an electric field at the interface, undergoing a drift process in which holes and electrons recombine, leaving ionized dopant atoms behind. This creates a space charge region, which is known as the depletion region.

An iso-type homojunction is a material junction where the crystalline bulk is identical on either side of the junction in crystallographic orientation and dopant material, but not in dopant quantity. This type of junction results in a diffusion action of FCCs. Under the assumption that the dopant atoms are fixed to their original positions in the crystal lattice, a lack of FCCs in the high concentration region and an excess of FCCs in the low concentration region creates a space charge region. Since this process is driven by diffusion, it is also known as the carrier diffusion region. The space charge region left by the diffusion process creates an electric field that opposes continuing diffusion, eventually stopping the diffusion process with an equal drift process. Unlike the aniso-type homojunction, the iso-type homojunction includes both carrier drift and diffusion processes. Consequently, mathematical modeling of the iso-type homojunction is complicated.

FCCs are most sensitive to imposed slowly-varying electric fields, therefore long-wavelength based electromagnetic investigation techniques are useful tools for FCC characterization. Initial attempts to measure the FCC concentration profiles of iso-type homojunctions involved time-domain based terahertz (THz) spectroscopy experiments in transmission configuration. These experiments have measured FCC concentrations of single crystals, but determination of complex layered structure properties is still a challenge [4,5]. Transmission techniques are limited by plasma absorption in the THz spectral region. This absorption is found in materials with large FCC densities. We present THz and mid-infrared (MIR) reflection type ellipsometric measurements as an optical, non-destructive, non-contact method of determining the FCC concentration profile and thickness parameters of homojunction bounded epilayers. Reflection configuration ellipsometry has been shown as a dependable technique for measuring FCC properties of layered semiconductor structures in the MIR and THz spectral range [6–9].

* Corresponding author.
E-mail address: alex.boosalis@huskers.unl.edu (A. Boosalis).

0040-6090/$ – see front matter © 2010 Elsevier B.V. All rights reserved.
doi:10.1016/j.tsf.2010.11.092

2. Theory

2.1. Iso-type homojunction FCC model

Initial attempts at mathematically defining the diffused FCC profile of an iso-type homojunction involve the Poisson equation coupled with the semiconductor current density equation based on drift and diffusion which results in a non-linear second order differential equation:

$$\underbrace{-\frac{d}{dx}\left[\frac{\mu_N D_N}{n(x)}\frac{d}{dx}n(x)\right]}_{\text{drift and diffusion equation}} = \overbrace{\frac{d}{dx}E(x) = \left[\frac{N_D(x)-n(x)}{\varepsilon_0\varepsilon}\right]}^{\text{Poisson's equation}}, \quad (1)$$

where $E(x)$ is the electric field in terms of the one dimensional depth x. The one dimensional depth is oriented perpendicular to the junction plane. The electron mobility is represented by μ_N, and ε_0 and ε are the vacuum and material dielectric constants, respectively. Eq. (1) is given only for electrons and makes two assumptions. First, the net current density is zero. Second, $N_D(x)$ and $n(x)$ describe the ionized dopant and FCC distributions on both sides of the iso-type homojunction. Eq. (1) shows that a changing FCC concentration ($n(x)$) creates a space charge region identified in Poisson's equation by the difference between $N_D(x)$ and $n(x)$. This space charge must be balanced by a free charge carrier diffusion (with diffusion constant D_N, diffusion is represented by $D_N \frac{d}{dx}n(x)$), and a FCC drift ($1/n(x)$). A general analytical solution for $n(x)$ is not available, thus most solution attempts revolve around numerical analysis [10,11]. Since a numerical analysis is difficult to implement in ellipsometric data modeling, an alternative approach must be considered.

An alternative, in depth, analytical analysis of the isotype homojunction problem was given by Kuznicki [12]. Kuznicki's approach assumes that the semiconductor material is non-degenerate and therefore $n(x)$ follows an energetic Boltzmann distribution. Rather than incorporating the drift and diffusion directly, the spatial FCC distribution is linked to the electric potential statistically:

$$n(x) = N_D \exp\left[q\phi(x)/kT\right], \quad (2)$$

where $\phi(x)$ is the electric potential, q is the elementary charge, k is the Boltzmann constant, and T is the temperature. The results are two independent formulae for $n(x)$ on each side of the assumedly abrupt iso-type homojunction. The high-doped FCC density profile is given by:

$$n_H(x, L_H) = N^+ \exp\left[\left(-\frac{\ln(N^+/N^-)}{1+\sqrt{N^+/N^-}}\right)\exp(x/L_H)\right], \quad (3)$$

where N^+ is the ionized dopant concentration of the high-doped side, N^- is the ionized dopant concentration of the low-doped side, and L is a characteristic charge screening length. The low-doped FCC density profile is governed by a similar formula comprised of the same parameters:

$$n_L(x, L_L) = N^- \exp\left[\ln\left(\frac{N^+}{N^-}\right) - 2\ln\left(\exp\left[0.5\left(1-\frac{N^-\ln(N^+/N^-)}{N^+-N^-}\right)\right] + x/L_L\right)\right]. \quad (4)$$

In order to employ the Eqs. (2), (3), and (4) the following assumptions from Ref. [12] must be met:

1. Free charge carrier diffusion is limited to one dimension.
2. Every semiconductor layer is non-degenerate.
3. $N_D(x)$ is an abrupt Heaviside expression with the higher side N^+ and the lower side N^-.
4. There is no dopant atom diffusion, i.e. the abrupt iso-type homojunction always occurs at $x=0$.
5. $N^+ \gg N^-$, with at least $N^+/N^- > 7$.

2.2. Aniso-type homojunction FCC model

In the aniso-type homojunction interface region, only the FCC depletion width needs to be considered. The depletion region width (d_{dep}) can be calculated with the well known depletion approximation model (i.e., the box model) [13], using the FCC concentrations as parameters:

$$d_{dep} = \left[\frac{2\varepsilon\varepsilon_0 kT}{q^2}\left(\frac{N^- + P}{N-P}\right)\ln\left(\frac{N^-P}{n_i^2}\right)\right]^{\frac{1}{2}}, \quad (5)$$

where P is the hole concentration in the P-type Si epitaxial layer and n_i is the intrinsic FCC concentration of Si.

2.3. Ellipsometry

For isotropic media, ellipsometry determines the ratio ρ of the complex-valued Fresnel reflection coefficients r_p and r_s for light polarized parallel p and perpendicular s to the plane of incidence, respectively. Commonly, ρ is presented in terms of the ellipsometric angles Ψ and Δ where:

$$\rho = r_p/r_s = \tan\Psi e^{i\Delta}, \quad (6)$$

[9,14,15]. In general, a stratified layer analysis of experimentally determined Ψ- and Δ-spectra is required in order to determine the complex valued dielectric functions of the sample constituents. The dielectric function of each sample constituent provides access to their Drude model free-charge-carrier parameters [9].

Parameter extraction from ellipsometric measurement is dependent on a lineshape analysis based on the physical models described in previous sections. Analysis requires varying the input parameters to produce a lowest possible mean squared error (MSE) between experimental data and model functions. Importance is placed on achieving a unique MSE, requiring comparison between alternative physical models and sufficient variation of input parameters in each model to verify a lowest possible MSE.

2.4. Model dielectric function

The FCC contribution to the dielectric function ($\varepsilon(\omega)$) is expressed by the Drude approximation, which modifies the static Si material dielectric constant ($\varepsilon_{DC}=11.7$):

$$\varepsilon(\omega) = \varepsilon_{DC} - \frac{nq^2}{\varepsilon_0 m(\omega^2 + i\omega\mu m/q)}, \quad (7)$$

where ω is the incident light angular frequency, q is the elementary charge, m is the effective mass, and μ is the mobility. In order to separate μ and m from n, effective mass parameters were assumed to be 0.26 m_e for electrons and 0.37 m_e for holes (where m_e is the free electron mass)[5]. The mobility (μ) was calculated from n using a simple model described by Jacoboni et al. using the model parameters determined in their original paper [16]:

$$\mu = \mu_{min} + \frac{\mu_{max}-\mu_{min}}{1+\left(\frac{n}{N_{ref}}\right)^{\alpha}}, \quad (8)$$

Table 1
Best-match model (lowest MSE) and spreading resistance parameters of the $N^+/N/P$ Si sample.

	Best-match	Spreading resistance
$P\ 10^{14}\ cm^{-3}$	1.89 ± 0.67	2.77
$N^-10^{15}\ cm^{-3}$	3.85 ± 0.17	3.81
$N^+10^{18}\ cm^{-3}$	1.68 ± 0.004	1.57

where $\mu_{min} = 92\ cm^2/Vs$, $\mu_{max} = 1360\ cm^2/Vs$, $N_{ref} = 1.3 \times 10^{17}\ cm^{-3}$, and $\alpha = 0.91$ for electrons; and $\mu_{min} = 47.7\ cm^2/Vs$, $\mu_{max} = 495\ cm^2/Vs$, $N_{ref} = 6.3 \times 10^{16}\ cm^{-3}$, and $\alpha = 0.76$ for holes.

3. Experiment

We investigate a sample composed of a heavily-doped *n*-type Si substrate followed by a low-doped *n*-type Si epitaxial layer (approximately 15 μm thick) and a low-doped *p*-type Si epitaxial layer (approximately 60 μm thick). This sample will be referred to in the following as the $N^+/N/P$ Si homojunction. The as-grown sample parameters and best-model values are summarized in Table 1.

Spectroscopic ellipsometry (SE) measurements were carried out in the THz and MIR spectral range at two different angles of incidence $\Phi_a = 50^\circ$ and 70°. We employed two different instruments for the measurements shown here. A commercially available MIR spectroscopic ellipsometer (J.A. Woollam Co. Inc.) and a custom built THz ellipsometer. Further details on the specifications of the THz ellipsometer and its operation can be found in Ref. [17].

4. Results

The THz- and MIR-SE data are presented in Fig. 1. The spectral range from 10 to 20 THz is dominated by Fabry–Pérot interference oscillations which decay towards higher frequencies. In the spectral range from 0.2 to 1.0 THz we observe two strong resonances at $\nu = 0.29$ THz and 0.89 THz. These resonances are attributed to the excitation of surface guided waves (SGW) with TE (electric field vector parallel to the interface) radiation fields [18]. The position, amplitude, and broadening of the surface guided waves are extremely sensitive to the free-charge carrier profiles within the sample [17].

The THz- and MIR-SE data were analyzed using a 5 phase optical model (see top of Fig. 2). In addition to the substrate and the two epitaxial layers, extended interface regions have to be included in the model. The resulting FCC profile is depicted in Fig. 2.

The interface region between N^+-Si substrate and *N*-Si epilayer (a.k.a. the diffusion region) is governed by free-charge carrier diffusion and drift processes which are analytically incorporated in the layer optical model as described in Section 2.1. The resulting spatially asymmetric FCC profile is approximated by a discrete variation of the free-charge carrier concentration and mobility within 250 sub-layers with abrupt interfaces. The abrupt interface between the N^+-Si substrate and the *N*-Si epilayer is the location of $x = 0$, where $n_H(x,L_H) = n_L(x,L_L)$. Negative *x* values lie in the substrate, where Eq. (3) governs the divergence of the FCC concentration from the substrate value N^+ over 50 sub-layers. Positive *x* values lie in the epilayer, where Eq. (4) represents the accumulation of FCCs diffusing from the substrate in excess of N^- over 200 sub-layers. The overall thickness of the interface region is determined by the parameters L_H and L_L, as only one thickness value allows $N^+ = n_H(-\infty, L_H)$ and $N^- = n_L(\infty, L_L)$.

The interface region between the *N*-Si epilayer and the *P*-Si epilayer (a.k.a the depletion region) is modeled with the depletion approximation (i.e. the box model) where it is assumed all FCCs have recombined leaving a space charge region. Electric charge in this region does not contribute to the Drude approximation, as all ionized dopant atoms are assumed to be spatially fixed (see Section 2.1). The width of this region is calculated from the FCC concentrations of the bounding interface layers (i.e. N^- and *P*) as described by Eq. (5).

The best-match model calculated parameters, as depicted in Fig. 2 are: $N^+ = (1.68 \pm 0.005) \times 10^{18}\ cm^{-3}$, $L_H = (3.18 \pm 0.004)$ nm, $L_L = (120 \pm 0.1)$ nm, $N^- = (3.85 \pm 0.17) \times 10^{14}\ cm^{-3}$, $d_N = (40.1 \pm 2.9)$ μm, $P = (1.89 \pm 0.67) \times 10^{14}\ cm^{-3}$, and $d_P = (29.9 \pm 2.9)$ μm.

5. Discussion

The application of our optical model results in an excellent agreement between best-match calculated and experimental data shown in Fig. 2. The best-match model parameters and spreading resistance values are compared in Table 1. We find excellent agreement

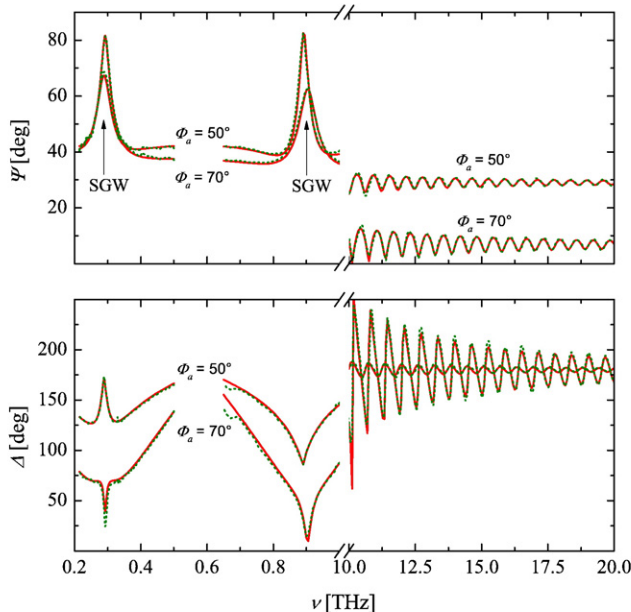

Fig. 1. Experimental (dotted lines) and calculated model (solid lines) Ψ and Δ spectra at 50° and 70° angles of incidence for a N^+/N/P sample. Data above 20 THz continues with the Fabry–Pérot interference pattern but was omitted for brevity.

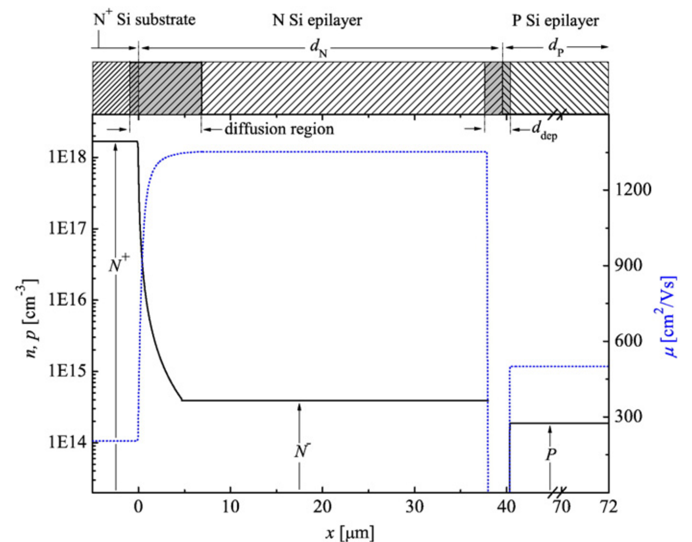

Fig. 2. FCC concentration (black line) and mobility (blue dotted line) profile as a function of *x*. Profiles were calculated from best-match model values of the FCC concentration, the characteristic charge screening length, and epilayer thickness. The uppermost bar shows the sample structure. A break in the graph was included to show the entire *P*-Si epilayer.

between FCC concentration parameters determined by best-match model analysis and spreading resistance FCC concentration ranges for all sample constituents. Accurate N^+/N/P sample analysis relies heavily on the correct description of the diffusion region. A symmetric diffusion profile model, as implemented in our previous work (see Ref. [6]), was rejected because it leads to a higher MSE values and does not provide access to important structural parameters, e.g., the location of the abrupt dopant junction. The asymmetric FCC diffusion profile model contains only physical parameters (e.g. the Debye lengths, active dopant concentrations) and allows the determination of the abrupt isotype homojunction location. Consequently, the asymmetric FCC diffusion model can accurately describe the thickness of the *N*-Si epilayer, a requirement under the assumption of plane parallel interfaces between sample layers (see Section 2.3). Non-contact, non-destructive measurement of the abrupt isotype homojunction location and its spatial relationship to diffusion FCCs can also be useful for improving the fabrication process of iso-type homojunction devices, and is only limited by assumptions (3) and (4) in Section 2.1.

The ability to distinguish between FCC concentration profiles is ascribed to the THz measurement. The SGW modes measured in the THz region are bound to the iso- and aniso-type interfaces, and are comprised of evanescent transverse electric waves. SGW dispersion is obtained from the s-polarized light reflectance (r_s) which is dependent on the depth profile of the dielectric function and the total thickness of the epilayer (see Eqs. (6) and (7)) [9,18]. This sensitivity to carrier concentration and thickness is exploited in our current model analysis.

While the current model accurately describes the N^+/N/P sample structure within current instrument precisions, further work is required to improve model accuracy and validate model physics. Specifically, the model ignores potential dopant diffusion at the iso-type homojunction and assumes perfect FCC recombination at the aniso-type homojunction. Spreading resistance measurement values provide a verification of best-match model parameters. Future work will include additional isotype homojunction samples to verify FCC diffusion asymmetry.

6. Conclusions

We have demonstrated optical measurements of the electrical and structural properties of a complex semiconductor epilayer structure. Application of an analytical model for iso-type and aniso-type homojunctions to data obtained from multiple ellipsometers covering a wide spectral range from 0.2 to 50 THz at multiple angles of incidence allows determination of FCC depth profiles in the diffusion and depletion regions. Comparison of best-match calculated data to spreading resistance measurement values reveals excellent agreement with expected sample properties.

Acknowledgements

The authors would like to acknowledge the financial support from the Army Research Office (D. Woolard, contract number W911NF-09-C-0097), the National Science Foundation (MRSEC DMR-0820521, MRI DMR-0922937, and DMR-0907475), the University of Nebraska-Lincoln, and the J.A. Woollam Foundation.

References

[1] K. Hayata, M. Koshiba, J. Appl. Phys. 77 (1995) 1808.
[2] S. Manipatruni, Q. Xu, M. Lipson, Opt. Express 15 (2007) 13035.
[3] H.X. Yuan, A.G.U. Perera, J. Appl. Phys. 79 (1996) 4418.
[4] M. Herrmann, M. Tani, K. Sakai, R. Fukasawa, J. Appl. Phys. 91 (2002) 1247.
[5] M. van Exter, D. Grischkowsky, Appl. Phys. Lett. 56 (1990) 1694.
[6] T. Hofmann, C.M. Herzinger, T.E. Tiwald, J.A. Woollam, M. Schubert, Appl. Phys. Lett. 95 (2009) 032102.
[7] T.E. Tiwald, D.W. Thompson, J.A. Woollam, W. Paulson, R. Hance, Thin Solid Films 313–314 (1998) 661.
[8] T.E. Tiwald, D.W. Thompson, J.A. Woollam, J. Vac. Sci. Technol. B 16 (1998) 312.
[9] M. Schubert, Infrared Ellipsometry on semiconductor layer structures: Phonons, plasmons and polaritons, Springer Tracts in Modern Physics, Vol. 209, Springer, Berlin, 2004.
[10] N. Haegel, A. White, Infrared Phys. 29 (1989) 915.
[11] P.E. Schmidt, M. Octavio, R.C. Callarotti, H.K. Henisch, J. Appl. Phys. 53 (1982) 4996.
[12] Z.T. Kuznicki, J. Appl. Phys. 69 (1991) 6526.
[13] R.F. Pierret, Semiconductor Device Fundamentals, Prentice Hall, 1996.
[14] R.M. Azzam, N.M. Bashara, Ellipsometry and Polarized Light, North-Holland Publ. Co., Amsterdam, 1984.
[15] H. Fujiwara, Spectroscopic Ellipsometry, John Wiley & Sons, New York, 2007.
[16] C. Jacoboni, C. Canali, G. Ottaviani, A.A. Quaranta, Solid State Electron. 20 (1977) 77.
[17] T. Hofmann, C.M. Herzinger, A. Boosalis, T.E. Tiwald, J.A. Woollam, M. Schubert, Rev. Sci. Instrum. 81 (2010) 023101.
[18] M. Schubert, T. Hofmann, J. Šik, Phys. Rev. B 71 (2005) 35324.